Author Manuscript

Author Manuscript

Author Manuscript

Author Manuscript

HHS Public Access

Author manuscript

Cell Mol Bioeng. Author manuscript; available in PMC 2016 September 01.

Published in final edited form as:

Cell Mol Bioeng. 2015 September 1; 8(3): 333–348. doi:10.1007/s12195-015-0397-4.

Smooth Muscle Stiffness Sensitivity is Driven by Soluble and Insoluble ECM Chemistry

William G. Herrick[1], **Shruti Rattan**[2], **Thuy V. Nguyen**[1], **Michael S. Grunwald**[1], **Christopher W. Barney**[3], **Alfred J. Crosby**[2], and **Shelly R. Peyton**[1]

[1]Department of Chemical Engineering, University of Massachusetts, 686 N. Pleasant Street, 159 Goessmann Laboratory, Amherst, MA 01003, USA

[2]Polymer Science and Engineering Department, University of Massachusetts, Conte Polymer Research Center, 120 Governors Dr., Amherst, MA 01003, USA

[3]Department of Materials Engineering, Purdue University, West Lafayette, USA

Abstract

Smooth muscle cell (SMC) invasion into plaques and subsequent proliferation is a major factor in the progression of atherosclerosis. During disease progression, SMCs experience major changes in their microenvironment, such as what integrin-binding sites are exposed, the portfolio of soluble factors available, and the elasticity and modulus of the surrounding vessel wall. We have developed a hydrogel biomaterial platform to examine the combined effect of these changes on SMC phenotype. We were particularly interested in how the chemical microenvironment affected the ability of SMCs to sense and respond to modulus. To our surprise, we observed that integrin binding and soluble factors are major drivers of several critical SMC behaviors, such as motility, proliferation, invasion, and differentiation marker expression, and these factors modulated the effect of stiffness on proliferation and migration. Overall, modulus only modestly affected behaviors other than proliferation, relative to integrin binding and soluble factors. Surprisingly, pathological behaviors (proliferation, motility) are not inversely related to SMC marker expression, in direct conflict with previous studies on substrates coupled with single extracellular matrix (ECM) proteins. A high-throughput bead-based ELISA approach and inhibitor studies revealed that differentiation marker expression is mediated chiefly *via* focal adhesion kinase (FAK) signaling, and we propose that integrin binding and FAK drive the transition from a migratory to a proliferative phenotype. We emphasize the importance of increasing the complexity of *in vitro* testing platforms to capture these subtleties in cell phenotypes and signaling, in order to better recapitulate important features of *in vivo* disease and elucidate potential context-dependent therapeutic targets.

Address correspondence to Shelly R. Peyton, Department of Chemical Engineering, University of Massachusetts, 686 N. Pleasant Street, 159 Goessmann Laboratory, Amherst, MA 01003, USA. speyton@ecs.umass.edu.

ELECTRONIC SUPPLEMENTARY MATERIAL

The online version of this article (doi:10.1007/s12195-015-0397-4) contains supplementary material, which is available to authorized users.

CONFLICT OF INTERESTS

William G. Herrick, Shruti Rattan, Thuy V. Nguyen, Michael S. Grunwald, Christopher W. Barney, Alfred J. Crosby, and Shelly R. Peyton declare no conflicts of interest. No human studies were carried out by the authors for this article. No animal studies were carried out by the authors for this article.

Author Manuscript Author Manuscript Author Manuscript Author Manuscript

Keywords

Extracellular matrix; Mechanobiology; Poly(ethylene glycol); Hydrogel; Atherosclerosis

INTRODUCTION

SMCs play an important role in the pathogenesis of atherosclerosis, the primary cause of heart disease and stroke. If stimulated during disease, these otherwise quiescent, immobilized, and contractile cells will degrade their surrounding ECM and invade developing plaques, where they rapidly proliferate and secrete ECM proteins, initiating a positive feedback loop, and contributing to arterial stiffening.

Of major interest to this field are the effects of substrate compliance on cellular behaviors relevant to the disease, such as proliferation and migration. These characteristics are most commonly investigated with biocompatible hydrogels that have control over both modulus and cell adhesion.[17,28,34,42,47] With these *in vitro* model systems, some common trends have emerged. Typically, cell proliferation is positively correlated with substrate compliance, both for SMCs[33,35] and other cells.[15] ECM proteins and other adhesive ligands, in concert with substrate elasticity, also regulate proliferation and migration of SMCs[13,14,28,34] and their sensitivity to soluble factors.[42,44,49] Despite their simplistic design, these *in vitro* systems have revealed substantial and important information about the effects of environmental factors on cellular phenotype.

Though the majority of literature in this field has consensus, there is some conflict and ambiguity among *in vitro* studies, and, separately, many *in vitro* studies do not recapitulate, or in some cases, directly conflict with *in vivo* studies.[9,12,20,22,39] As one example, SMC proliferation and motility are typically inversely related to expression of protein markers *in vitro* and *in vivo*, but conflicting reports[9,12,20] raise serious questions regarding the true diversity of SMC phenotypes and the interrelation between the extracellular environment, phenotype, and pathological behaviors.

Broadly, we hypothesize that these literature disagreements are due to significant differences between human biology, *in vitro* models, and *in vivo* animal models. The *in vivo* arterial microenvironment is complex and heterogeneous, and we hypothesize that a lack of recapitulation of this ECM complexity may be partially to blame for conflicts between *in vitro* and *in vivo* findings. Further, SMCs themselves reside on a spectrum of phenotypes, yet only two phenotypes are typically described: in a healthy, intact arterial media, SMCs are differentiated and ‘contractile’, whereas proliferative SMCs in an atherosclerotic lesion are the dedifferentiated, ‘synthetic’ phenotype. In response, we investigated SMC phenotypic diversity with a polymeric biomaterial system designed to capture the intersection of physical, chemical, and mechanical signals in the microenvironment. We used poly (ethylene glycol) dimethacrylate-phosphorylcholine (PEG-PC) hydrogels[18,32] that we recently developed as a tunable biomaterial substrate, and coated them with mixtures of integrin-binding ECM proteins representative of ECM evolution in a vessel during plaque formation. We forced SMCs into the contractile phenotype chemically, and then quantified their plasticity toward the synthetic phenotype as modulated by substrate stiffness, integrin

Author Manuscript Author Manuscript Author Manuscript Author Manuscript

binding, and soluble factors. With this subtly more complex system, we were better able to see this spectrum of SMC phenotypes, which we found was driven by FAK, phosphatidylinositol 3-kinase (PI3K), and Akt signaling. This study represents an early step towards closer replication of the *in vivo* microenvironment, and we hope our work will inspire others to carefully consider the effects of numerous relevant stimuli on SMC behavior, with any tunable platform.

MATERIALS AND METHODS

Cell Culture

All reagents were from Life Technologies (Carlsbad, CA), unless otherwise noted. Human aortic smooth muscle cells(SMCs) from passages 2 through 8 were cultured in Medium 231 supplemented with smooth muscle growth supplement (SMGS) and 1% penicillin–streptomycin (P/S). For experiments, medium was changed to DMEM with 10% FBS. Cells were synched into the contractile phenotype with serum starvation for 48 h, and stimulation with 2.5 ng/mL recombinant human TGFβ_1 (R&D Systems, Minneapolis, MN) for an additional 48 h.

PEG-PC Hydrogel Polymerization and Contact Mechanics Measurements

PEG-PC polymer hydrogels were prepared on methacrylate-functionalized 15 mm coverslips (Thermo Fisher Scientific, Waltham, MA) as previously described.[18,32] To quantify the elastic moduli of the hydrogels directly on the coverslips, a piezo-controlled linear actuator (Burleigh Inchworm Nanopositioner) was used to bring a polystyrene-coated steel cylindrical probe (cross-sectional radius ~0.75 mm) into contact with a sample. Upon contact and reproach, the relative displacement, δ, and resulting force, P, were measured with a custom-designed load cell (Fig. 1a). In addition, the contact radius, a, established between the probe and the gel was confirmed to equal the radius of the probe with a Zeiss Axiovert 200 M microscope (Carl Zeiss, Oberkochen, Germany). Tests were conducted at a crosshead speed of 0.5 μm/s and the total displacement for each test was fixed at 30 μm. Linearity of the force–displacement curve was also confirmed for a crosshead speed of 0.1 μm/s (Suppl. Fig. 1).

To quantify the elastic modulus, the compliance, $C=\frac{\partial \delta}{\partial P}$, was determined from the linear force–displacement curves (Fig. 1a), and the modulus, E, determined by[40]:

$$E=\frac{(1-v^2)}{2Ca}\left\{1+1.33\left(\frac{a}{h}\right)+1.33\left(\frac{a}{h}\right)^3\right\}^{-1}$$

where $\frac{a}{h}$ is the ratio of the contact radius to the thickness of the hydrogel. However, a direct calculation of the Young's modulus requires independently determining the Poisson ratio, v, and thus we report an effective modulus, $E^*=\frac{E}{1-v^2}$, in Fig. 1. Conveniently, fully swollen hydrogels are typically considered to be incompressible under relevant time scales of loading[2] with Poisson ratios in the range of 0.4–0.5. Therefore, to facilitate comparisons with other reports, we also present these mechanical results in Fig. 1 as Young's moduli, E,

Author Manuscript Author Manuscript Author Manuscript Author Manuscript

with an assumed Poisson's ratio of $\nu = 0.5$, and we refer to these values throughout the remainder of the text.

Protein Functionalization to Hydrogel Surfaces

Two protein cocktails were prepared in PBS (Figs. 1c and 1d): 'BaM' (basement membrane representation) containing 50% (w/v) collagen IV (recombinant human; Sigma-Aldrich) and 50% laminin (mouse), and 'InF' (inflammatory ECM representation) containing 50% monomeric collagen I (rat tail) and 50% fibronectin (human plasma; EMD Millipore, Billerica, MA). Glacial acetic acid was added to the InF cocktail at 0.14 vol.% to prevent collagen fibril formation.

Hydrated gels were treated with sulfo-SANPAH (0.3 mg/mL in pH 8.5 HEPES buffer; ProteoChem, Denver, CO) under UV light for 10 min at ~3 in. They were then washed with PBS 2× and incubated with 75 μL of cocktail for a 3 $\mu g/cm^2$ theoretical surface concentration. After 20 h, gels were transferred to fresh wells, washed 3× over 30 min in PBS, and UV sterilized for at least 30 min prior to cell seeding.

Cell Proliferation Assays

SMCs were seeded onto gels (~5600 cells/cm^2), and the initial cell populations were assessed 24 h post-seeding, then once more after they were synched into the contractile phenotype and stimulated for 96 h with either SMDS- or SMGS-containing DMEM ('differentiation medium' and 'growth medium,' respectively). AlamarBlue was used to quantify relative cell numbers, using fluorescence (λ_{ex} = 550 nm, λ_{em} = 585 nm) measured with a Spectramax M5 microplate reader (Molecular Devices, Sunnyvale, CA). Results are reported as the fold-difference between the first and final days, from a minimum of 5 biological replicates per condition.

Cell Migration and Invasion Assays

For motility assays, cell-seeded hydrogels were immobilized in the wells of 24-well plates with 5-min epoxy (Devcon, Danvers, MA) following phenotype synching and treated with either differentiation or growth medium. Cell migration was quantified by recording *x*–*y* positions with a Zeiss Axio Observer Z1 (Carl Zeiss) in brightfield for 12 h at 15 min intervals. Cell positions were manually tracked with ImageJ using the Manual Tracking plugin, and we calculated the average velocity, displacement, and chemotactic index of each tracked cell by fitting to a random walk model in MATLAB with code provided by Aaron Meyers (MIT, Whitehead Institute). The results are reported as the average cell speed and chemotactic index, from a minimum of 3 independent biological replicates and 100 cells per condition.

For invasion assays, 300 μL 3 mg/mL collagen I gels (rat tail) were polymerized directly on cell-seeded gels following phenotype synching, in the presence of either differentiation or growth medium. Cells were allowed to invade into the collagen gels for 4 days, and then imaged with a Zeiss Axio Observer Z1 with 30 μm Z-slices. The results are reported as the average cell invasion depth, from a minimum of 3 independent biological replicates and 140

Author Manuscript Author Manuscript Author Manuscript Author Manuscript

invaded cells per condition (with the exception of two biological replicates of the soft BaM condition in differentiation medium).

SMC Marker Western Blotting

SMCs on gels (~11,000 cells/cm^2) were lysed using ice-cold Tris-Triton lysis buffer (10 mM Tris, pH 7.4, 100 mM NaCl, 1 mM EDTA, 1 mM EGTA, 1% Triton X-100, 10% glycerol, 0.1% SDS, 0.5% deoxycholate) with freshly added protease inhibitors (cOmplete Mini EDTA-free protease inhibitor tablets; Roche Applied Sciences, Penzberg, Germany). Sample protein concentrations were measured with the Pierce BCA assay (Thermo Fisher) and a BioTek ELx800 absorbance microplate reader (BioTek, Winooski, VT), normalized, boiled with Laemmli buffer, separated on 4–20% Tris–glycine polyacrylamide gels and transferred to PVDF membranes *via* Western blotting. SMC markers were detected with primary antibodies for calponin (clone EP798Y, 1:10000; Abcam, Cambridge, MA) and smoothelin-B (clone H-300, 1:200; Santa Cruz Biotechnology, Dallas, TX), with cyclophilin B as an internal control (1:10,000, Thermo Fisher). Bands were visualized with HRP secondary antibodies and enhanced chemiluminescence using a Syngene G:Box.

Characterization of SMC Morphology

Sparsely seeded SMCs were fixed with 4% formaldehyde, blocked with 5% bovine serum albumin (BSA) in Tris-buffered saline with 0.1% Triton-X100 (TBS-T), and stained with Cellomics Whole Cell Stain Blue (Thermo Fisher) for 90 min according to the manufacturer's instructions. Imaging was performed with a Zeiss Axio Observer Z1 at ×10 magnification. Individual cells were manually traced in ImageJ and characterized with the built-in "Measurement" tool. The results are reported here as average cell properties from at least 3 independent biological replicates and 100 cells per condition.

To visualize focal adhesions and actin stress fibers, cells were rinsed 2× with warm PBS, fixed in fresh 4% formaldehyde, and blocked with AbDil (2% BSA in TBS-T). Vinculin was immunofluorescently labeled with a monoclonal mouse anti-vinculin antibody (Sigma-Aldrich) and an anti-mouse FITC secondary antibody (Jackson ImmunoResearch Laboratories, West Grove, PA). F-actin was fluorescently labeled with Alexa Fluor 555-conjugated phalloidin, and cell nuclei were labeled with DAPI (MP Biomedicals, Santa Ana, CA). Antibody incubations were performed for 1 h in AbDil, in the dark, and cells were thoroughly washed between labeling steps with TBS-T. Each sample was equilibrated with ProLong Gold antifade reagent for 5 min before imaging. Images were taken with a 63× oil immersion lens on a Zeiss Axio Observer Z1 microscope, and ImageJ (NIH, Bethesda, MD) was used to adjust the brightness and contrast for clarity in figures. In separate experiments, calponin and smoothelin were stained in the same manner using the antibodies also used for Western blotting and an Alexa Fluor 444 conjugated secondary antibody for visualization.

Cell Signaling Time Course with MAGPIX Multiplexing

A MAGPIX (Luminex Corporation, Austin, TX) and cell signaling multiplex assay kit (48–680MAG; Merck Millipore, Billerica, MA) was used to measure the activities of nine phospho signaling proteins (CREB, ERK, NFκB, JNK, p38, p70 S6 K, STAT3, STAT5 and Akt) during 3 separate time courses: (1) directly during seeding onto biomaterial surfaces,

Author Manuscript Author Manuscript Author Manuscript Author Manuscript

(2) during TGFβ_1 treatment after 48 h of serum starvation, and (3) during stimulation with differentiation medium. Only those signaling molecules that showed significant changes are reported. Lysis was performed with MAGPIX lysis buffer (50 mM Tris–Cl, pH 7.1, 1% NP-40, 10% glycerol, and 150 mM NaCl) with freshly-added phosphatase inhibitors (Phosphatase Inhibitor Cocktail II, 2× working concentration; Boston BioProducts) and protease inhibitors (cOmplete Mini, EDTA-free), plus (all from Thermo Fisher Scientific) additional sodium pyrophosphate (1:100 from 0.1 Mstock), β-glycerophosphate (1:40 from 1 M stock), PMSF (1:500 from 0.5 M stock), leupeptin (1:1000 from 10 mg/mL stock) and pepstatin A (1:1000 from 5 mg/mL stock). The MAGPIX assays were performed according to the manufacturer's instructions. The results are reported here as the average net mean fluorescence intensity (Net MFI) of 2–4 biological replicates per condition and time point.

Kinase Inhibition Experiments

SMCs (~11,000 cells/cm^2) were serum starved for 48 h, then kinase inhibitors were co-administered with TGFβ_1 as described above. Akt was inhibited with sc-66 at 1 μg/mL (20 mg/mL stock in DMSO; Abcam) for 1 h, FAK with FAK inhibitor 14 at 100 μM (100 mM stock in DMSO; Merck Millipore) for the duration of the experiment, and PI3K with LY294002 at 50 μM (50 mM stock in DMSO; Merck Millipore) for 1 h. After 48 h the samples were lysed and Western blotted for calponin and smoothelin, as described above.

Statistical Analysis

Statistical analysis was performed using Prism v5.04 (GraphPad Software, La Jolla, CA) and the Real Statistics Resource pack software (Release 3.5). Copyright (2013–2015) Charles Zaiontz. www.real-statistics.com. Data are reported as mean ± standard error, unless otherwise noted. Statistical significance of mean differences was evaluated with an unpaired Student's *t* test, and two-way ANOVAs with 1 fixed factor were performed where noted. Two-factor ANOVA (*via* regression) analysis of collagen invasion depth data (due to the large number of data points), and three-factor ANOVA (*via* regression) analysis of invasion and proliferation data sets were performed using the Real Statistics Resource Pack. $p \leq 0.05$ is denoted with *, ≤0.01 with **, ≤0.001 with *** and ≤0.0001 with ****; $p>0.05$ was considered not significant ('ns').

RESULTS

PEG-PC Hydrogels are Highly Tunable and Capable of Supporting SMC Differentiation

We used indentation to quantify the effective modulus of samples that were prepared identically to those used in biological experiments. As expected for a linear elastic material loaded with a flat punch geometry, the relationship between force and displacement is linear for all compositions and the two crosshead speeds tested (Figs. 1a–1c, 0.5 μm/s, and Suppl. Fig. 1, 0.1 μm/s). We found that the slopes of these curves generally increases with crosslinker (PEGDMA) concentration, which indicates an increasing stiffness possibly due to the formation of a denser network, as previously described.[18] To create a biomaterial environment that captured key biochemical and physical environments, we coupled the tunable mechanics of the PEG-PC gel system with ECM proteins representative of the proteins to which SMCs are attached in a healthy medial layer (basement membrane, or

Author Manuscript Author Manuscript Author Manuscript Author Manuscript

BaM), or those representative of an inflammatory plaque (inflammatory or InF) (Fig. 1d). These insoluble cues were combined with soluble factors also commonly found in these two scenarios. In all ensuing experiments, SMCs were seeded onto gel surfaces with defined modulus and integrin-binding proteins, serum-starved, and finally treated with TGFβ_1 to prime the cell culture into a differentiated, "contractile" state on day 5 (Fig. 1e).

Integrin Binding Regulates SMC Proliferative Response to Soluble Factors

We quantified the proliferation of initially contractile SMCs on gels from 40 to 94 kPa, after 4 days of culture in growth or differentiation medium (Figs. 2a and 2b) and found that the InF ECM promotes a higher rate of proliferation in combination with differentiation medium than does the BaM ECM, but in growth medium the difference in means were not statistically significant at each stiffness level. Modulus generally had a positive effect on proliferation, with the exception of proliferation on the InF ECM in differentiation medium. This effect was most pronounced with the combination of the BaM ECM and differentiation medium (Fig. 2b). Substrate modulus had a less pronounced effect on proliferation on the InF configuration with growth medium, and played no significant role with differentiation medium.

Three-factor ANOVA analysis found that medium type was the single largest driver of proliferation (23% of total variance, $p<0.0001$), followed by modulus (9%, $p<0.001$) and ECM (6%, $p<0.001$). Intriguingly, while we did find that the interaction between ECM and medium was significant, the effect on total variance was small (1.8%, $p<0.05$). This result is counter to our initial conclusions from visual inspection of the data, and it is possible that the large contribution of random error to the total variance may be obfuscating the strength of the interaction between ECM and medium in the ANOVA analysis.

However, when we considered the data sets for each ECM composition independently and performed two-way ANOVAs comparing medium and modulus, we found that medium had a larger effect on total variance with BaM ECM (30% of total variance from medium, $p<0.0001$) than with InF (19% from medium, $p<0.0001$), which agrees with visual inspection. This conclusion is further corroborated by the finding that, when proliferation in each medium is analyzed independently, ECM is a significant factor in differentiation medium, but not growth medium (28.5 vs. 1.5% of total variance, with $p<0.0001$ and $p = 0.25$ for differentiation and growth medias, respectively). Taken together, we conclude from these results that soluble factor sensitivity is dependent on integrin-ECM interactions, in agreement with a previous study comparing fibronectin, collagen, and laminin-coated gels.[38] Heparin is well known to inhibit the effects of certain growth factors on SMC proliferation[8,25] further supporting this hypothesis. However, the soluble factors in growth medium are apparently capable of overriding any growth inhibitory effects mediated by the BaM ECM, resulting in no apparent ECM-specific differences in proliferation with this condition.

Integrin Binding is the Most Significant Driver of Both 2D and 3D Motility

As models of the early stages of SMC invasion into a developing plaque, we evaluated both the 2D random migration and 3D invasiveness of SMCs as modulated by the various

Author Manuscript Author Manuscript Author Manuscript Author Manuscript

physical and chemical factors in our system (Figs. 2c–2f). We found that ECM and medium type had a very significant impact on average cell speeds and migration directionality (Figs. 2c and 2d). SMC speed has been reported as biphasic with respect to substrate modulus,[34] which we did not observe in our initial experiments; however, after introducing an even softer condition (11 kPa), we found that cells on BaM in differentiation medium migrated much slower than the other stiffnesses, demonstrating that the biphasic regime for BaM and differentiation medium was not spanned in our original experiments (not shown). Unexpectedly, the average speed on BaM is significantly higher than on InF with either medium supplement, but the chemotactic index on InF is higher. This latter result indicates that cells on BaM migrated erratically and non-directionally. Growth medium generally increased both random migration speed and the chemotactic index on both ECMs. We quantified the effects of these 3 factors with ANOVA analyses: when considering each factor level independently and applying two-factor ANOVA with the remaining factors, we found significant interactions between all factor pairs ($p<0.0001$), but the effects were weak (1–12% of total variance from interactions, average 4.8%). On the whole, ECM was the most significant factor affecting migration speed (88, 53, 76, and 86% of total variance at each increasing stiffness level, $p<0.0001$ for all), and the medium type had a greater effect on migration speed on InF ECM than on BaM (9 vs. 1%, $p<0.0001$). The effect of modulus, however, was modest, never exceeding 4% of total variance. Very similar trends and effects were found with the chemotactic index data.

Given these surprising results on 2D surfaces, we hypothesized that integrin binding was significantly influencing cell adhesion, and could therefore impact 3D invasion as well. With a collagen gel invasion assay, we found that SMC invasion depth is greater from the BaM ECM in growth medium, with a modest increase in invasion depth from soft vs. stiff substrates (Figs. 2e and 2f). Invasion depth in differentiation medium was overall shallow, but greater for the soft BaM condition. Given the observed weaker adhesion/spreading on BaM, it is possible that invasion depth is greater due to ease of detachment; however, since the SMCs are given 4 days to invade the collagen matrix, BaM may also induce phenotypic changes that affect the SMCs long after leaving the BaM surface. Interestingly, as with migration speed, we found with three-factor ANOVA (*via* regression) that medium and ECM significantly affected invasion depth, but unlike with migration speed, the effect of medium was greater (13 vs. 8.5%, $p<0.0001$). Similarly, modulus only weakly affected invasion depth (2% of variance, $p<0.0001$). When we analyzed the growth medium data independently with two-factor ANOVA, the ECM type accounted for 14% of the total variance ($p<0.0001$) in this medium type, and stiffness for <3% ($p<0.0001$), with no significant interaction. Taken together, we conclude that ECM is the major determinant of SMC 2D migration characteristics and a significant factor in collagen invasion, but medium has the greatest impact on invasive properties.

Since SMC phenotype is reported to be correlated with cell shape and size,[24] we quantified morphology on our various surfaces (Figs. 3a and 3b). We found that cells are approximately two–threefold larger in area on InF compared to BaM, consistent with a synthetic phenotype on these inflammatory proteins. Average cell aspect ratio (AR) was used to evaluate the ‘spindle’-like shape of SMCs, with high ARs indicating an elongated,

Author Manuscript Author Manuscript Author Manuscript Author Manuscript

spindle-like morphology, indicative of the contractile phenotype. We found that the average cell AR has little dependence on modulus or ECM after synching (Suppl. Fig. 2), which is further validation that this priming step does chemically "sync" the otherwise heterogeneous cells into a consistent, differentiated cell population, even though they are seeded onto different stiffness gels with different integrin-binding conditions. Remarkably, we observed that the average AR of cells on BaM in growth medium increases with substrate modulus, and it is higher overall than on InF with either growth or differentiation medium stimulation. Thus, although ARs are synched during TGFβ_1 treatment, this contractile phenotype appears to be better maintained, at least with respect to cell morphology, on stiff gels with basement membrane proteins, regardless of the ensuing medium conditions. We have visualized these morphological differences with immunofluorescent staining in Fig. 3c.

Stiffness and Soluble Factors Modulate Marker Expression

To connect SMC motility and proliferation to prototypical markers of SMC differentiation, we evaluated the expression of calponin and smoothelin *via* Western blotting (Figs. 4a and 4c). Synthetic SMCs secrete ECM and are classically characterized by the downregulation of several marker proteins (caldesmon, calponin, SM-MHC, smoothelin, and more[45,46,48]). These proteins interact with the actin cytoskeleton and have roles in regulating actomyosin contractility, and are therefore involved in mechanotransduction. In agreement with previous reports,[16] we found that treatment with TG-Fβ_1 during the synching steps dramatically increased expression of both calponin and smoothelin following serum starvation. The differentiation medium supplement (SMDS) is intended to promote SMC differentiation, while the growth medium induces proliferation and dedifferentiation. In agreement with these expectations, we found that, relative to TGFβ_1 treatment, calponin expression is modestly up- and down-regulated by differentiation and growth medium, respectively (Figs. 4a and 4c). Smoothelin expression, however, increases slightly with differentiation and *further* increases with growth medium (Figs. 4c and 4d). Calponin expression also increases somewhat on stiff, InF-coated substrates with differentiation medium, but is not affected by stiffness in the other contexts, whereas smoothelin expression is enhanced on stiff substrates with TGFβ_1 and differentiation medium, or with growth medium on InF. While the effect of stiffness was modest overall, it was most pronounced in combination with InF, and expression of both markers was greater on InF than BaM on soft substrates. In fact, though these expression patterns were consistently observed, we believe it is actually the relative *lack* of substantial differences in expression across conditions after synching that is the most intriguing conclusion derived from these results. This is in spite of some major differences in cell behaviors (Fig. 2), a finding that *directly contradicts* the notion that SMC marker expression and pathological behaviors indicative of the synthetic phenotype are inversely related.

Given the reported scarcity of smoothelin in cultured SMCs,[45] we visualized actin fibers with calponin or smoothelin *via* immunofluorescence (Figs. 4b, 4d). These results confirmed antibody specificity for stress-fiber localized proteins and co-localization of smoothelin to the nucleus.[43] Since the robust expression of smoothelin we observed was unexpected, we confirmed expression of the smoothelin-B mRNA with reverse transcriptase PCR in SMCs grown on TCPS in FBS-containing growth medium (Fig. 4e).

Author Manuscript Author Manuscript Author Manuscript Author Manuscript

FAK Controls SMC Plasticity, in Part Through PI3K/Akt

To understand the possible signaling mechanisms driving the phenotypic diversity of the SMCs we had observed thus far, we quantified the activation of several major signaling proteins during adhesion, TGFβ_1 treatment, and stimulation with differentiation medium, using a phospho-protein multiplex assay (Fig. 5). We observed characteristic spikes in phosphorylation of ERK and Akt on each modulus tested, and phosphorylation was generally higher on the InF ECM (Fig. 5a). We observed minimal to no phosphorylation of Akt during TGFβ_1 stimulation (not shown), and ERK again peaked at early time points and was enhanced on the InF surfaces. Interestingly, ERK phosphorylation was greater on the stiffer hydrogel during TGFβ_1 stimulation (Fig. 5b). Finally, we saw Akt and ERK activities diverge during stimulation with differentiation medium (Fig. 5c). Akt appears to be suppressed with differentiation, and recovers after 24 h, whereas ERK is again stimulated during the medium change. We see, again, that the phosphorylation of both these proteins is higher on the InF surface with minimal modulus-dependent effects.

We then performed experiments with inhibitors to signaling proteins that are associated both with Akt and integrin activity to draw a connection between our observed SMC phenotypes and ECM composition (Fig. 5d). We found that FAK was the strongest up-stream driver of SMC differentiation on all conditions. In fact, inhibition of FAK completely abrogated expression of both calponin and smoothelin (Fig. 5d). However, while inhibition of PI3K or Akt reduced expression of calponin, it had little to no effect on smoothelin expression. Interestingly, though we did not find any substantial differences in expression between the two protein cocktails, it is of note that cells on InF remained well-spread and appeared relatively normal over 48 h, but cells on the BaM ECM undergo rounding and detachment, prohibiting us from obtaining data for the 40 kPa BaM condition with Akt or FAK inhibitors. These results imply that regulation of smoothelin and calponin expression diverges down-stream of activated FAK, though PI3K and Akt may still play a smaller role. We also investigated the impact of ERK and Akt inhibition on proliferation outcomes, but Akt inhibition for 96 h (with inhibitor reapplied at 48 h) caused total cell loss through detachment and/or apoptosis under all conditions, and ERK inhibition had inconsistent, statistically insignificant effects (Suppl. Fig. 3).

DISCUSSION

We designed a 2D biomaterial system that reflects several major, physicochemical changes in the *in vivo* extracellular microenvironment that are purported to occur during the progression of atherosclerosis and restenosis. Our observations demonstrate that interplay between the various components of a complex microenvironment modulate phenotype and behavior in complicated, unexpected ways. In fact, many assumptions from the SMC literature on/in other *in vitro* environments do not hold here, which we suspect is due to the focus on single physicochemical cues, instead of the combinatorial approach we have taken here.

One surprising aspect revealed by our data is that expression of SMC marker proteins is not inversely related to pathological behaviors associated with the synthetic phenotype (i.e., proliferation and motility) as commonly reported.[5,6,9,13,39] In fact, expression of calponin,

Author Manuscript Author Manuscript Author Manuscript Author Manuscript

and smoothelin to a lesser extent, were higher in SMCs on soft substrates with inflammatory rather than basement membrane proteins. In contrast, proliferation was significantly greater on InF than BaM in differentiation medium, whereas motility was significantly greater on BaM. While this latter observation does hint at an inverse relationship between marker expression and migration speed, expression is only higher with InF on the soft condition. This suggests that the relationship between marker expression and pathological behaviors is variable and inconsistent, and that the signaling pathways regulating SMC proliferation and motility are not strictly antagonistic to those regulating marker expression, or possibly even coupled at all. However, the proliferation trends in differentiation medium indicate that the effects of soluble factors in these contexts are modulated by integrin activity.[19,21]

In agreement with expected effects of these ECM proteins on SMC phenotype, we found that both medias induced a contractile, spindle-shaped morphology on BaM and a large, rhomboidal shape associated with the synthetic phenotype on InF (Fig. 3 and Suppl. Fig. 2). Remarkably, these traits did not correspond to substantial differences in expression of calponin or smoothelin, despite their purported status as components of the SMC contractile apparatus. Of equal interest is the observation that migration and invasion characteristics are disconnected from SMC marker expression. However, upon further reflection, the invasion from the BaM ECM towards growth medium models the process of detachment from the basement membrane and migration towards chemo attractants in a developing plaque (Figs. 2e and 2f). Therefore, we speculate that SMCs in this model may be reflective of an invasive phenotype characteristic of the early stages of atherosclerosis. Finally, our initial experiments showed that the effect of stiffness on 2D migration speed did not follow the previously reported biphasic trend *in vitro*.[34] We initially explained this by our multiple ECM protein approach, as this previous study was done on pure fibronectin, and collagen IV has been previously reported to strongly enhance SMC motility relative to the other ECM proteins used here.[31] We investigated this further by performing additional migration experiments with BaM on 11 kPa PEG-PC in differentiation medium, and possibly identified the range of elastic moduli over which SMCs migrate biphasically in this microenvironment.

Measurement of several signaling protein activity levels over time implicates Akt and ERK1/2 signaling pathways in regulating these phenomena, the activities of which are overall greater on InF than BaM (Fig. 5). Increased stiffness also enhanced signaling under certain conditions, but relatively modestly. This analysis was followed up with kinase inhibition experiments to identify potential connections between cell signaling pathways and integrins/focal adhesion complexes. The effects of Akt and FAK inhibitors were similar on soft BaM during TGFβ_1 treatment, with total loss of cells by 48 h, but PI3K inhibition only caused significant rounding. Cell rounding was also dramatic with all inhibitors on stiffer BaM, but cells were not completely detached. Remarkably, inhibitors had little visible effect with InF during TGFβ_1 treatment, with the interesting exception that FAK inhibition dramatically reduced cell–cell contacts (not shown).

We also measured the effect of kinase inhibition during TGFβ_1 treatment on marker expression and, despite apparently significant effects on the actin cytoskeleton and/or adhesion structures, were surprised to find little relation between markers and attachment/

Author Manuscript Author Manuscript Author Manuscript Author Manuscript

rounding. The most intriguing finding is that FAK inhibition completely abrogates expression of both markers, implicating FAK as a key regulator of contractile marker expression in 2D. Furthermore, expression of calponin and smoothelin appear to be regulated by distinct, but possibly overlapping signaling pathways that diverge downstream of FAK. This conclusion is derived from the finding that smoothelin is modestly affected by PI3K inhibition, but barely affected by Akt inhibition, whereas calponin is strongly downregulated by inhibition of either on BaM. On InF, however, calponin is more strongly regulated *via* Akt than PI3K, which further indicates that Akt may be activated through ILK instead of PI3K.

The likely explanation of how integrin binding in our system regulated stiffness and medium condition sensitivity is crosstalk between integrin binding and colocalized growth factors. Numerous studies (for review, see Ref. 37) have reported a concomitant increase in migration and proliferation after treatment with soluble factors or mechanical stimulation, and our data agrees with this notion. However, it has long been hypothesized that migration and proliferation of synthetic SMCs in atherosclerosis are temporally distinct phenomena.[7,26] We believe this seeming contradiction between *in vitro* data and physiological intuition is an illustrative example of the limitations necessarily imposed by simpler models. Our data indicates that, as the ECM surrounding SMCs changes from a basement membrane composition to that found in a plaque, there is a switch from migratory behavior to a high rate of proliferation. This data altogether is *in vitro* evidence that proliferation and migration may be inversely related *with respect to particular ECM compositions*, a conclusion that fits well with our understanding of the pathology of atherosclerosis.

From our data and previous work, we propose a hypothetical signaling pathway diagram in Fig. 6 that may explain the impact of ECM composition on SMC phenotype and behaviors, and how these processes are modulated by soluble factors. As described above, our inhibitor experiments indicate that FAK regulates the expression of SMC markers, and suggest that calponin and smoothelin regulation may diverge downstream of FAK. These experiments also indicate that calponin expression may be mediated primarily *via* PI3K/Akt on BaM and ILK/Akt on InF, whereas smoothelin may be regulated *via* disparate, or possibly partially overlapping pathways. We additionally propose that activation of different integrin heterodimers—most likely $\alpha_V\beta_3$ on InF and $\alpha_2\beta_1$ on BaM—well explains the physiologically relevant phenomena we observed. The much greater spreading area and slower migration of SMCs on InF, as well as a higher prevalence of stress fibers and vinculin-rich focal adhesions, is an indicator of significant FAK autophosphorylation,[36] which in turn may recruit and activate c-Src and enhance overall FAK signaling.[30] In fact, β_3 integrin itself provides Src homology 2 (SH2) binding domains for direct association of c-Src independent of actin and focal adhesion assembly.[3] The higher prevalence of these signaling motifs on InF may lead to greater proliferation by accumulated signaling through the c-Src/ERK1/2 and/or FAK/ILK/Akt pathways, and greater spreading through FAK-mediated enhancement of RhoA/ROCK and stress fiber formation. In contrast, while $\alpha_2\beta_1$ integrin activation on BaM is likely to generate many of the same signaling patterns,[19] the

Author Manuscript Author Manuscript Author Manuscript Author Manuscript

weaker adhesion we observed suggests lower FAK/c-Src signaling, resulting in dampened proliferation.

We also propose a mechanism that explains our observed ECM-controlled switch from a migratory to a proliferative phenotype. Prior work with fibroblasts revealed that these cells are motile and proliferative at low and high concentrations of PDGF, respectively, a switchover mediated by clathrin-mediated endocytosis (CME) and raft/caveolin-mediated endocytosis (RME).[10] We hypothesize that this switching of endocytic mechanisms could also be induced by changes in integrin activation. This proposal fits well with the finding that migration is random and non-directional on BaM, as CME is responsible for rapid, localized recycling of growth factor receptors at the plasma membrane, which enables a fast cellular response to transient microgradients of chemoattractants.[11] The adhesion properties on BaM also suggest faster turn-over of FAs, which is likely to support rapid migration on soft substrates. This latter mechanism would seem to also apply to $\alpha_2\beta_1$ integrin binding to monomeric collagen I on InF, but this is likely mitigated by the additional presence of fibronectin, which has been found to dramatically increase phosphorylation of paxillin,[4] decrease migration, and increase spreading.[1]

Soluble factors play a role in these phenomena by activating integrin-associated growth factor receptors, which further enhance mitogenic signaling *via* c-Src and/or Akt. Despite the relative scarcity of soluble factors in differentiation medium, proliferation is greater on InF due possibly to overall greater basal activation of mitogenic signaling induced by ligand-free association of integrins and GFRs. Other possible contributory factors include the induction of autocrine growth factor production by heparin[41] or collagen I,[23] supported by our finding that Akt activity increased after 24 h in differentiation medium on the stiff condition. Proliferation is lower on BaM, however, due to a lack of many of these effects and/or potential sequestration of TGFβ_1 in the pericellular matrix by collagen IV,[27] which has been shown to potentiate the growth factor inhibition of heparin.[29] Finally, despite the lack of significance between the fold-change in cell populations, we propose that SMCs on InF in growth medium actually proliferate more than on BaM due to the mechanisms described above, but this is obfuscated by the greater spreading and attachment of SMCs, resulting in faster saturation of the surface and cell–cell contact inhibition.

CONCLUSIONS

We present here a simple *in vitro* biomaterial system that can parse out the complexity of SMC phenotype and signalling while under multi-factorial exposure to differences in substrate modulus, integrin binding, and soluble factor stimulation. The novelty in our approach was initially synching cell populations on different surfaces, and then probing their susceptibility to the synthetic phenotype when dosed with different cocktails of soluble factors. This simple change from previous methods allowed us to see the true phenotypic diversity of SMCs and helped resolve some contradictions that exist between *in vitro* and *in vivo* studies. Coupled with our signalling analysis, we demonstrated that integrin binding is the overriding driver of SMC phenotype, and it dictated SMC sensitivity to soluble factors. This was modulated primarily by FAK phosphorylation, and we propose FAK's downstream targets are regulated by the specific activated integrin heterodimer and its ability to recruit

Author Manuscript Author Manuscript Author Manuscript Author Manuscript

growth factor receptors and Src into the focal adhesion complex. In sum, our results demonstrate the need to examine any biophysical cue in proper context, and studies of mechanosensing in isolation (including our own) may result in incomplete conclusions.

Supplementary Material

Refer to Web version on PubMed Central for supplementary material.

Acknowledgments

This work was supported by a Grant in Aid from the American Heart Association (13GRNT16190013), a Barry and Afsaneh Siadat Career Development Award, grants from the National Science Foundation and the National Cancer Institute (DMR-1234852 and DMR-1304724), start-up funds from the University of Massachusetts Amherst, and the UMass MRSEC on Polymers (DMR-0820506). WGH was supported by a fellowship from the Institute of Cellular Engineering IGERT at UMass (DGE-0654128). SRP is a Pew Biomedical Scholar supported by the Pew Charitable Trusts. We are also grateful to Dr. Nele Van Dessel for helpful discussions.

References

1. Abou Zeid N, Vallés A-M, Boyer B. Serine phosphorylation regulates paxillin turnover during cell migration. Cell Commun Signal. 2006; 4:8. [PubMed: 17121676]
2. Anseth KS, Bowman CN, Brannon-Peppas L. Mechanical properties of hydrogels and their experimental determination. Biomaterials. 1996; 17(17):1647–1657. [PubMed: 8866026]
3. Arias-Salgado EG, Lizano S, Sarkar S, Brugge JS, Ginsberg MH, Shattil SJ. Src kinase activation by direct interaction with the integrin beta cytoplasmic domain. Proc Natl Acad Sci USA. 2003; 100(23):13298–13302. [PubMed: 14593208]
4. Bellis S, Perrotta J, Curtis M, Turner C. Adhesion of fibroblasts to fibronectin stimulates both serine and tyrosine phosphorylation of paxillin. Biochem J. 1997; 381:375–381. [PubMed: 9230116]
5. Bjorkerud S. Effects of transforming growth factor-beta 1 on human arterial smooth muscle cells in vitro. Arterioscler Thromb Vasc Biol. 1991; 11(4):892–902.
6. Blank RS, Owens GK. Platelet-derived growth factor regulates actin isoform expression and growth state in cultured rat aortic smooth muscle cells. J Cell Physiol. 1990; 142(3):635–642. [PubMed: 2312620]
7. Bornfeldt KE. Intracellular signaling in arterial smooth muscle migration versus proliferation. Trends Cardiovasc Med. 1996; 6(5):143–151. [PubMed: 21232288]
8. Castellot JJ, Pukac LA, Caleb BL, Wright TC, Karnovsky MJ. Heparin selectively inhibits a protein kinase C-dependent mechanism of cell cycle progression in calf aortic smooth muscle cells. J Cell Biol. 1989; 109(6):3147–3155. [PubMed: 2592420]
9. Corjay MH, Thompson MM, Lynch KR, Owens GK. Differential effect of platelet-derived growth factor- versus serum-induced growth on smooth muscle alpha-actin and nonmuscle beta-actin mRNA expression in cultured rat aortic smooth muscle cells. J Biol Chem. 1989; 264(18):10501–10506. [PubMed: 2732233]
10. De Donatis A, Comito G, Buricchi F, Vinci MC, Parenti A, Caselli A, Camici G, Manao G, Ramponi G, Cirri P. Proliferation versus migration in platelet-derived growth factor signaling: the key role of endocytosis. J Biol Chem. 2008; 283(29):19948–19956. [PubMed: 18499659]
11. De Donatis A, Ranaldi F, Cirri P. Reciprocal control of cell proliferation and migration. Cell Commun Signal. 2010; 8:20. [PubMed: 20822514]
12. Desmouliere A, Rubbia-Brandt L, Gabbiani G. Modulation of actin isoform expression in cultured arterial smooth muscle cells by heparin and culture conditions. Arterioscler Thromb Vasc Biol. 1991; 11(2):244–253.
13. Engler A, Bacakova L, Newman C, Hategan A, Griffin M, Discher D. Substrate compliance versus ligand density in cell on gel responses. Biophys J. 2004; 86(1 Pt 1):617–628. [PubMed: 14695306]

Author Manuscript Author Manuscript Author Manuscript Author Manuscript

14. Gaudet C, Marganski WA, Kim S, Brown CT, Gunderia V, Dembo M, Wong JY. Influence of type I collagen surface density on fibroblast spreading, motility, and contractility. Biophys J. 2003; 85(5):3329–3335. [PubMed: 14581234]
15. Hadjipanayi E, Mudera V, Brown RA. Close dependence of fibroblast proliferation on collagen scaffold matrix stiffness. J Tissue Eng Regen Med. 2009; 3(2):77–84. [PubMed: 19051218]
16. Hautmann MB, Madsen CS, Owens GK. A transforming growth factor beta (TGFbeta) control element drives TGFbeta-induced stimulation of smooth muscle alpha-actin gene expression in concert with two CArG elements. J Biol Chem. 1997; 272(16):10948–10956. [PubMed: 9099754]
17. Hazeltine LB, Simmons CS, Salick MR, Lian X, Badur MG, Han W, Delgado SM, Wakatsuki T, Crone WC, Pruitt BL, Palecek SP. Effects of substrate mechanics on contractility of cardiomyocytes generated from human pluripotent stem cells. Int J Cell Biol. 2012; 2012:508294. [PubMed: 22649451]
18. Herrick WG, Nguyen TV, Sleiman M, McRae S, Emrick TS, Peyton SR. PEG-phosphorylcholine hydrogels as tunable and versatile platforms for mechanobiology. Biomacromolecules. 2013; 14(7):2294–2304. [PubMed: 23738528]
19. Hollenbeck ST, Itoh H, Louie O, Faries PL, Liu B, Kent KC. Type I collagen synergistically enhances PDGF-induced smooth muscle cell proliferation through pp60src-dependent crosstalk between the alpha2beta1 integrin and PDGF beta receptor. Biochem Biophys Res Commun. 2004; 325(1):328–337. [PubMed: 15522237]
20. Holycross BJ, Blank RS, Thompson MM, Peach MJ, Owens GK. Platelet-derived growth factor-BB-induced suppression of smooth muscle cell differentiation. Circ Res. 1992; 71(6):1525–1532. [PubMed: 1423945]
21. Ishigaki T, Imanaka-Yoshida K, Shimojo N, Matsushima S, Taki W, Yoshida T. Tenascin-C enhances crosstalk signaling of integrin $\alpha v\beta 3$/PDGFR-β complex by SRC recruitment promoting PDGF-induced proliferation and migration in smooth muscle cells. J Cell Physiol. 2011; 226(10): 2617–2624. [PubMed: 21792920]
22. Janat MF, Argraves WS, Liau G. Regulation of vascular smooth muscle cell integrin expression by transforming growth factor beta1 and by platelet-derived growth factor-BB. J Cell Physiol. 1992; 151(3):588–595. [PubMed: 1295906]
23. Jones JI, Prevette T, Gockerman A, Clemmons DR. Ligand occupancy of the alpha-V-beta3 integrin is necessary for smooth muscle cells to migrate in response to insulin-like growth factor. Proc Natl Acad Sci USA. 1996; 93(6):2482–2487. [PubMed: 8637900]
24. Li S, Sims S, Jiao Y, Chow LH, Pickering JG. Evidence from a novel human cell clone that adult vascular smooth muscle cells can convert reversibly between non-contractile and contractile phenotypes. Circ Res. 1999; 85(4):338–348. [PubMed: 10455062]
25. Lindner V, Olson NE, Clowes AW, Reidy MA. Inhibition of smooth muscle cell proliferation in injured rat arteries. Interaction of heparin with basic fibroblast growth factor. J Clin Invest. 1992; 90(5):2044–2049. [PubMed: 1430226]
26. Louis SF, Zahradka P. Vascular smooth muscle cell motility: from migration to invasion. Exp Clin Cardiol. 2010; 15(4):e75–e85. [PubMed: 21264073]
27. Macri L, Silverstein D, Clark RAF. Growth factor binding to the pericellular matrix and its importance in tissue engineering. Adv Drug Deliv Rev. 2007; 59(13):1366–1381. [PubMed: 17916397]
28. Mann B, West J. Cell adhesion peptides alter smooth muscle cell adhesion, proliferation, migration, and matrix protein synthesis on modified surfaces and in polymer scaffolds. J Biomed Mater Res. 2002; 60(1):86–93. [PubMed: 11835163]
29. McCaffrey TA, Falcone DJ, Brayton CF, Agarwal LA, Welt FG, Weksler BB. Transforming growth factor-beta activity is potentiated by heparin via dissociation of the transforming growth factor-beta/alpha 2-macroglobulin inactive complex. J Cell Biol. 1989; 109(1):441–448. [PubMed: 2473082]
30. Mitra SK, Schlaepfer DD. Integrin-regulated FAK-Src signaling in normal and cancer cells. Curr Opin Cell Biol. 2006; 18(5):516–523. [PubMed: 16919435]
31. Nelson PR, Yamamura S, Kent KC. Extracellular matrix proteins are potent agonists of human smooth muscle cell migration. J Vasc Surg. 1996; 24(1):25–32. [PubMed: 8691524]

Author Manuscript Author Manuscript Author Manuscript Author Manuscript

32. Nguyen TV, Sleiman M, Moriarty T, Herrick WG, Peyton SR. Sorafenib resistance and JNK signaling in carcinoma during extracellular matrix stiffening. Biomaterials. 2014; 35(22):5749–5759. [PubMed: 24726537]
33. Peyton SR, Kim PD, Ghajar CM, Seliktar D, Putnam AJ. The effects of matrix stiffness and RhoA on the phenotypic plasticity of smooth muscle cells in a 3-D biosynthetic hydrogel system. Biomaterials. 2008; 29(17):2597–2607. [PubMed: 18342366]
34. Peyton SR, Putnam AJ. Extracellular matrix rigidity governs smooth muscle cell motility in a biphasic fashion. J Cell Physiol. 2005; 204(1):198–209. [PubMed: 15669099]
35. Peyton SR, Raub CB, Keschrumrus VP, Putnam AJ. The use of poly(ethylene glycol) hydrogels to investigate the impact of ECM chemistry and mechanics on smooth muscle cells. Biomaterials. 2006; 27(28):4881–4893. [PubMed: 16762407]
36. Pirone DM, Liu WF, Ruiz SA, Gao L, Raghavan S, Lemmon CA, Romer LH, Chen CS. An inhibitory role for FAK in regulating proliferation: a link between limited adhesion and RhoA-ROCK signaling. J Cell Biol. 2006; 174(2):277–288. [PubMed: 16847103]
37. Rensen SSM, Doevendans PAFM, van Eys GJJM. Regulation and characteristics of vascular smooth muscle cell phenotypic diversity. Neth Heart J. 2007; 15(3):100–108. [PubMed: 17612668]
38. Sazonova OV, Isenberg BC, Herrmann J, Lee KL, Purwada A, Valentine AD, Buczek-Thomas JA, Wong JY, Nugent MA. Extracellular matrix presentation modulates vascular smooth muscle cell mechanotransduction. Matrix Biol. 2015; 41:36–43. [PubMed: 25448408]
39. Shi ZD, Abraham G, Tarbell JM. Shear stress modulation of smooth muscle cell marker genes in 2-D and 3-D depends on mechanotransduction by heparan sulfate proteoglycans and ERK1/2. PLoS One. 2010; 5(8):e12196. [PubMed: 20808940]
40. Shull KR, Ahn D, Chen WL, Flanigan CM, Crosby AJ. Axisymmetric adhesion tests of soft materials. Macromol Chem Phys. 1998; 199(4):489–511.
41. Skaletz-Rorowski A, Schmidt A, Breithardt G, Buddecke E. Heparin-induced overexpression of basic fibroblast growth factor, basic fibroblast growth factor receptor, and cell-associated proteoheparan sulfate in cultured coronary smooth muscle cells. Arterioscler Thromb Vasc Biol. 1996; 16(8):1063–1069. [PubMed: 8696947]
42. Stegemann JP, Nerem RM. Altered response of vascular smooth muscle cells to exogenous biochemical stimulation in two- and three-dimensional culture. Exp Cell Res. 2003; 283(2):146–155. [PubMed: 12581735]
43. Stephan S, Ball SG, Williamson M, Bax DV, Lomas A, Shuttleworth CA, Kielty CM. Cell-matrix biology in vascular tissue engineering. J Anat. 2006; 209(4):495–502. [PubMed: 17005021]
44. Ucuzian AA, Brewster LP, East AT, Pang Y, Gassman AA, Greisler HP. Characterization of the chemotactic and mitogenic response of SMCs to PDGF-BB and FGF-2 in fibrin hydrogels. J Biomed Mater Res Part A. 2010; 94(3):988–996.
45. van Eys GJ, Niessen PM, Rensen SS. Smoothelin in vascular smooth muscle cells. Trends Cardiovasc Med. 2007; 17(1):26–30. [PubMed: 17210475]
46. Winder SJ, Allen BG, Fraser ED, Kang HM, Kargacin GJ, Walsh MP. Calponin phosphorylation in vitro and in intact muscle. Biochem J. 1993; 296:827–836. [PubMed: 8280082]
47. Wong JY, Velasco A, Rajagopalan P, Pham Q. Directed movement of vascular smooth muscle cells on gradient-compliant hydrogels. Langmuir. 2003; 19(9):1908–1913.
48. Worth NF, Rolfe BE, Song J, Campbell GR. Vascular smooth muscle cell phenotypic modulation in culture is associated with reorganisation of contractile and cytoskeletal proteins. Cell Motil Cytoskelet. 2001; 49(3):130–145.
49. Zheng B, Duan C, Clemmons DR. The effect of extracellular matrix proteins on porcine smooth muscle cell insulin-like growth factor (IGF) binding protein-5 synthesis and responsiveness to IGF-I. J Biol Chem. 1998; 273:8994–9000. [PubMed: 9535886]

Author Manuscript Author Manuscript Author Manuscript Author Manuscript

Biography

Shelly R. Peyton is the Barry and Afsaneh Siadat Assistant Professor of Chemical Engineering at the University of Massachusetts, Amherst. She received her B.S. in Chemical Engineering from Northwestern University in 2002 and went on to obtain her MS and Ph.D. in Chemical Engineering from the University of California, Irvine. She was then an NIH Kirschstein post-doctoral fellow in the Biological Engineering department at MIT before starting her academic appointment at UMass in 2011. Her research interests are in biomaterial design and understanding how cell-material interactions contribute to cancer aggressiveness, cardiovascular disease progression, and regenerative medicine. Since arriving at UMass she has been named a Pew Biomedical Scholar, received a New Innovator Award from the NIH, and she was recently awarded a CAREER grant from the NSF.

Author Manuscript Author Manuscript Author Manuscript Author Manuscript

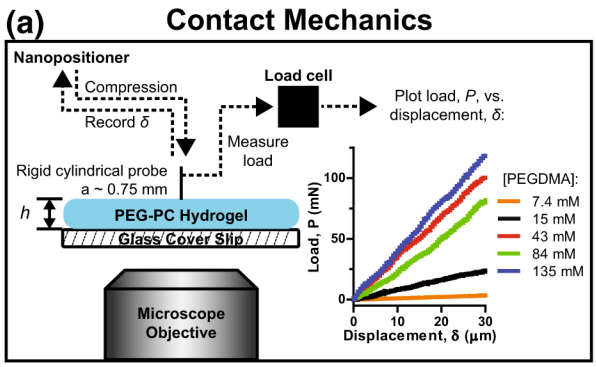

(c)

[PEG] (mM)	Effective E ± SD (kPa)	Young's E ± SD (kPa)
7.4	15 ± 2.7	11 ± 2.0
15	53 ± 1.9	40 ± 1.4
43	110 ± 2.3	80 ± 1.7
84	80 ± 3.3	60 ± 2.5
135	130 ± 7.6	94 ± 5.7

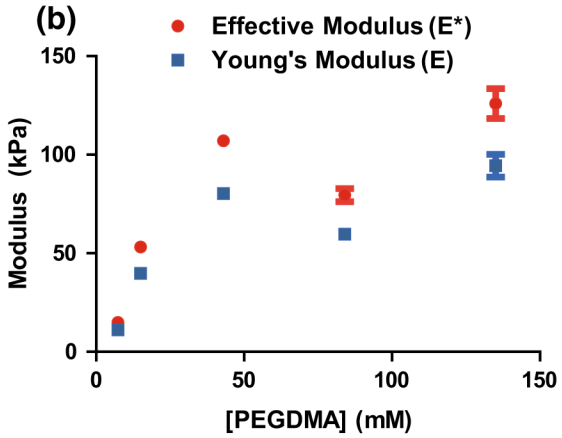

(d)

ECM	BaM	1.5 μg/cm^2 each: collagen IV, laminin
	InF	1.5 μg/cm^2 each: fibronectin, collagen I
Soluble Factors	Differentiation Media	30 μg/mL heparin, 1% FBS
	Growth Media	2 ng/mL bFGF, 0.5 ng/mL EGF, 5 ng/mL heparin, 2 μg/mL IGF-I, 0.2 μg/mL BSA, 4.9% FBS

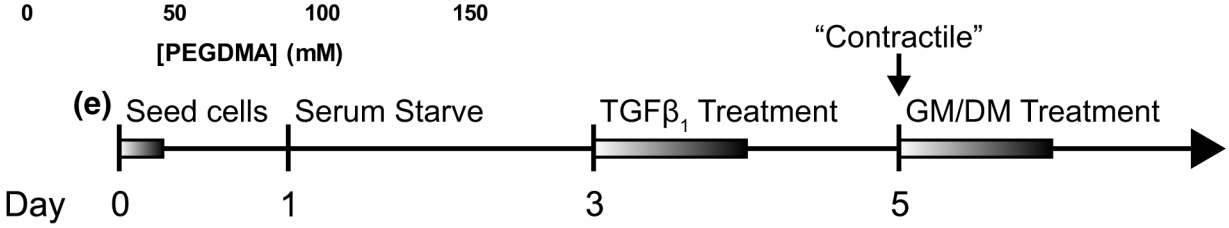

FIGURE 1.

PEG-PC hydrogels that mimic the *in vivo* microenvironment of SMCs. (a) PEG-PC hydrogel elastic modulus on glass coverslips was measured with contact mechanics by bringing a cylindrical probe into contact with the gel surface and measuring the force, *P*, vs. displacement, *δ*, with a displacement rate of 0.5 *μ*m/s. Data is plotted with compressive force and displacement values being positive (b) The effective modulus, E^*, was measured over a range of [PEGDMA] concentrations from a minimum of three samples per condition, and used to calculate a Young's modulus, *E*, with an estimated Poisson's ratio of 0.5. (c) PEG-PC mechanical data plotted as a function of crosslinker (PEGDMA) concentration. (d) Two different compositions of adhesive proteins and soluble factors were used to reflect changes in the arterial microenvironment. (e) Timeline of experiments. "Contractile" denotes phenotype synching; GM and DM are growth and differentiation mediums, respectively.

Author Manuscript Author Manuscript Author Manuscript Author Manuscript

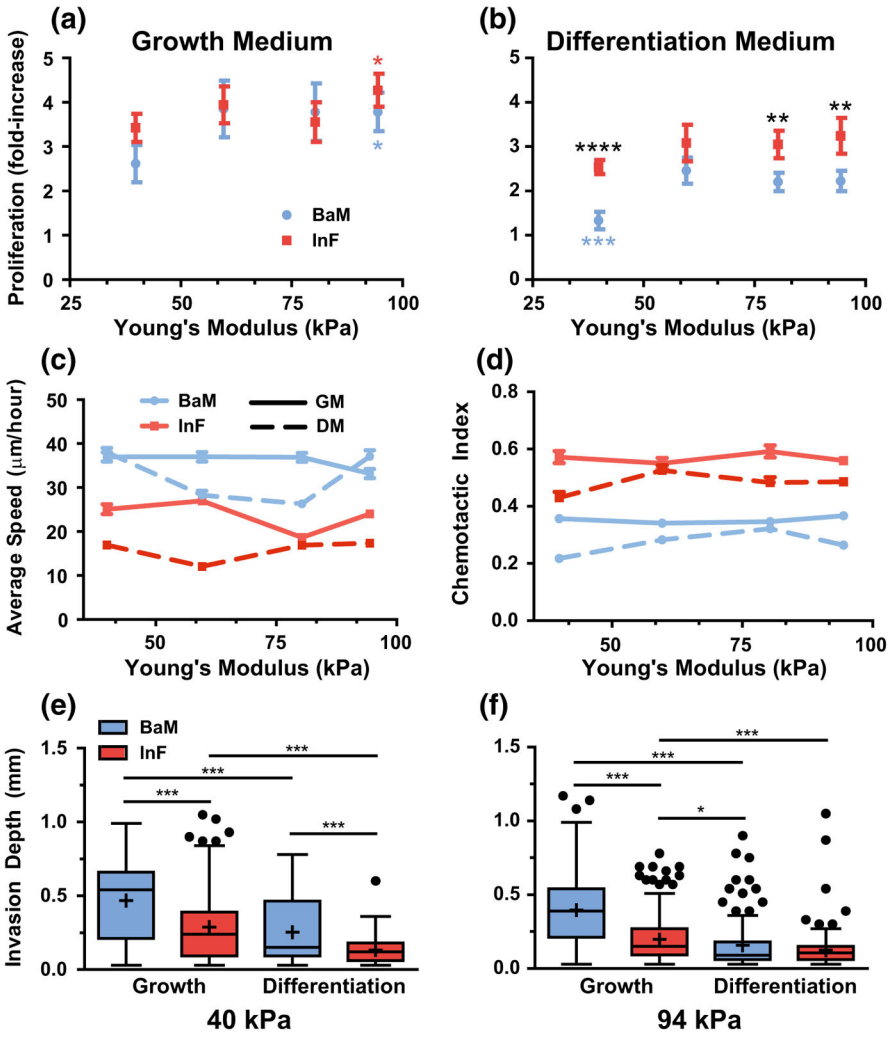

FIGURE 2.

Physicochemical effects on SMC growth and motility. (a, b) SMC proliferation at 4 days of culture was measured as a function of hydrogel modulus (*x*-axis), on either BaM (blue) or InF (red) proteins, and stimulation with either growth medium (a) or differentiation medium (b). An asterisk (*) indicates significantly different from softest condition. Black asterisks (*) indicate significance at that stiffness, blue asterisks (*) indicate significant difference from stiffer BaM conditions. Error bars are ± SEM with $N = 5–6$ independent biological replicates. (c, d) SMC migration speed (c) and chemotactic index (d) was quantified as a function of Young's modulus (*x*-axis) on the different integrin-binding proteins (colors) and stimulated with medium conditions (solid and dashed lines). Error bars are ±SEM with $N>100$ cells and at least 3 independent biological replicates. (e, f) In a collagen gel invasion assay, SMCs were seeded on two different stiffness gels, and on the two protein combinations (colors). Their invasion into an overlaid collagen gel was measured in both medium conditions (*x*-axis). Data is presented as Tukey box plots with $N>100$ cells from at least 3 independent biological replicates (with the exception of 2 independent replicates for soft BaM in differentiation medium.).

Author Manuscript Author Manuscript Author Manuscript Author Manuscript

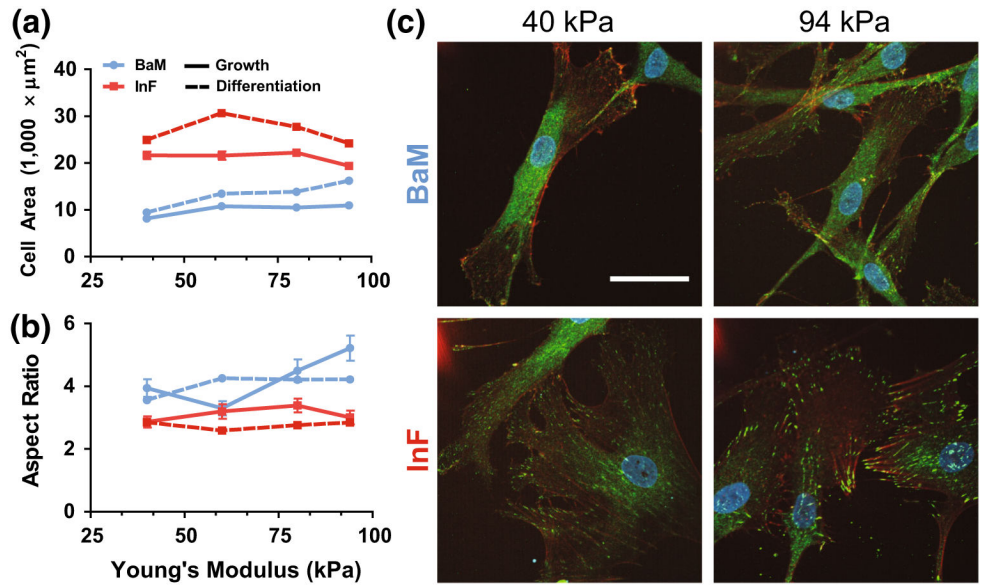

FIGURE 3.

SMC adhesion and morphology is affected by ECM. (a, b) Cell spread area (a) and aspect ratio (b) were quantified with manual tracing as a function of hydrogel modulus (*x*-axis) on each protein cocktail (colors) and medium condition (dashed and solid lines). Error bars are ±SEM with $N>100$ cells and 3 independent biological replicates. (c) Immunofluorescent staining of vinculin (green), actin stress fibers (orange), and nuclei (DAPI) of SMCs on two stiffness gels, on each integrin-binding condition, both in growth medium after 48 h of culture. Scale bar is 50 μm.

Author Manuscript Author Manuscript Author Manuscript Author Manuscript

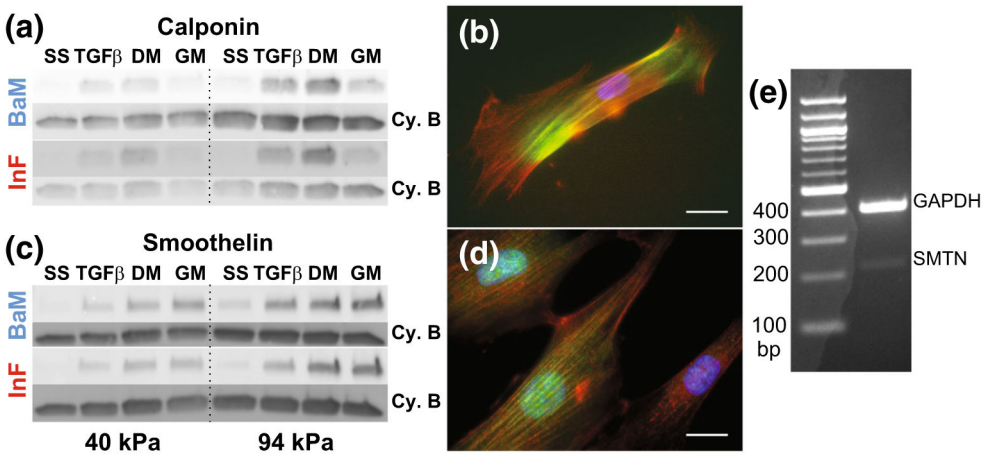

FIGURE 4.

Expression of calponin and smoothelin has greater dependence on soluble factors than ECM. Representative Western blots for calponin (a) and smoothelin (c) after each step of priming and stimulation with growth or differentiation medium. SS: Serum-starve, TGFβ: TGFβ_1 treatment step, DM: switch to differentiation medium, GM: switch to growth medium. Internal control bands for normalization are cyclophilin B (Cy. B). Immunofluorescent staining of calponin (b) and smoothelin (d) (green) with actin (red) and DAPI (blue). Scale bar is 50 μm. (e) Reverse transcriptase PCR to confirm expression of SMTN-B mRNA.

Author Manuscript Author Manuscript Author Manuscript Author Manuscript

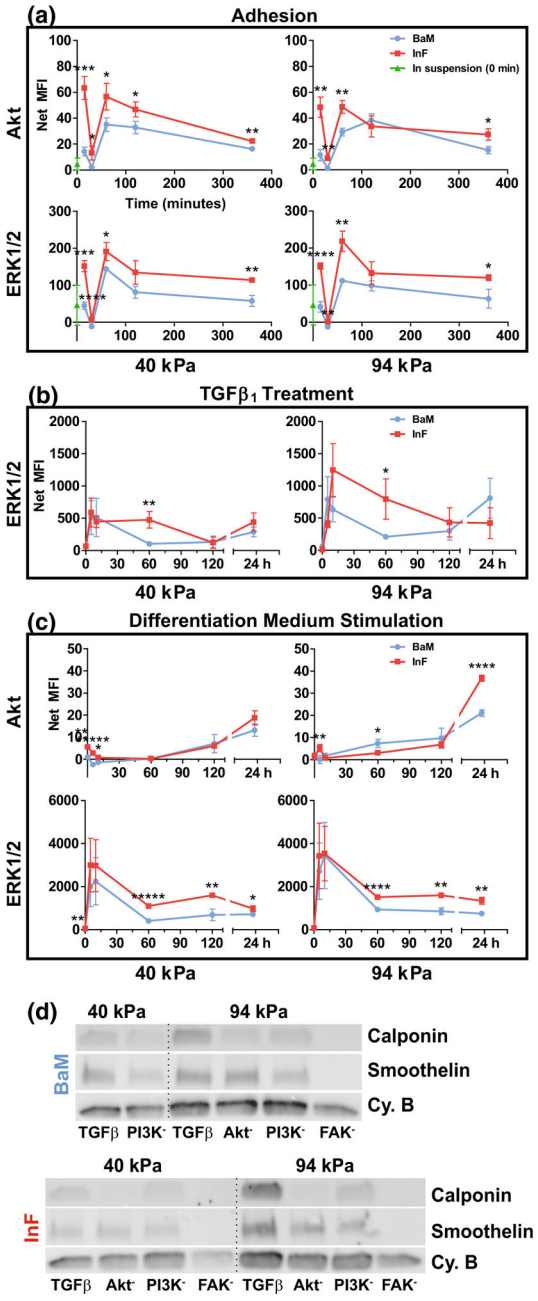

FIGURE 5.

InF proteins stimulate Akt and ERK/12 signaling. (a–c) Phosphorylation of Akt and ERK, when occurred, are plotted as a function of time (*x*-axis) directly upon adhesion to substrates (a), directly after TGFβ_1 stimulation (b), or upon changing to differentiation medium (c). Error bars are ±SEM from N = 2–4 independent biological replicates. (d) Western blotting of SMC markers with inhibited FAK, PI3K or Akt during TGFβ_1 treatment on two stiffnesses and on both protein mixtures. Internal control bands for normalization are cyclophilin B (Cy. B).

Author Manuscript Author Manuscript Author Manuscript Author Manuscript

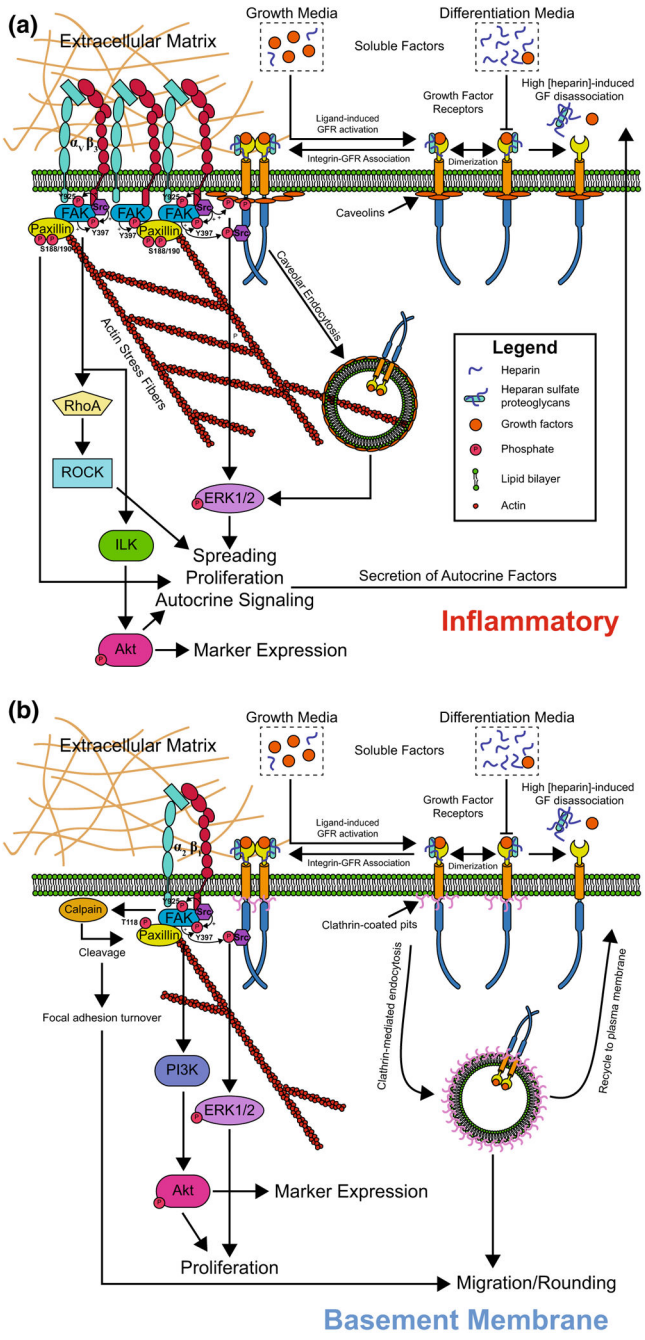

FIGURE 6.

Proposed mechanisms and signaling behind ECM-dependent behaviors. (a) Integrin ligation on InF, in particular $\alpha_V\beta_3$, promotes strong adhesion and spreading, FAK autophosphorylation, focal adhesion formation, FAK/ILK/Akt signalling to induce marker expression and/or proliferation, or c-Src localization and ERK1/2 signaling. Association of growth factor receptors (GFRs) with integrins may enhance proliferative signaling *via* c-Src. (b) On BaM, $\alpha_2\beta_1$ integrin is likely a key mediator of ECM-specific signaling. The

Author Manuscript Author Manuscript Author Manuscript Author Manuscript

prevalence of active FAK is overall lower, resulting in weaker adhesion, poor spreading, and rapid FA turnover, promoting migration.